Spatial Patterns in Urban Systems

Hoai Nguyen HUYNH[*,1,2,C], Evgeny MAKAROV[†3], Erika Fille LEGARA[‡1], Christopher MONTEROLA[§1,2], and Lock Yue CHEW[¶2,4]

[1]Institute of High Performance Computing, Agency for Science Technology and Research, Singapore
[2]Complexity Institute, Nanyang Technological University, Singapore
[3]Baseride Technologies, Singapore
[4]School of Physical and Mathematical Sciences, Nanyang Technological University, Singapore
[C]huynhhn@ihpc.a-star.edu.sg

ABSTRACT

Understanding the morphology of an urban system is an important step toward unveiling the dynamical processes of its growth and development. At the foundation of every urban system, transportation system is undeniably a crucial component in powering the life of the entire urban system. In this work, we study the spatial pattern of 73 cities across the globe by analysing the distribution of public transport points within the cities. The analysis reveals that different spatial distributions of points could be classified into four groups with distinct features, indicating whether the points are clustered, dispersed or regularly distributed. From visual inspection, we observe that the cities with regularly distributed patterns do not have apparent centre in contrast to the other two types in which star-node structure, *i.e.* monocentric, can be clearly observed. Furthermore, the results provide evidence for the existence of two different types of urban system: well-planned and organically grown. We also study the spatial distribution of another important urban entity, the amenities, and find that it possesses universal properties regardless of the city's spatial pattern type. This result has one important implication that at small scale of locality, the urban dynamics cannot be controlled even though the regulation can be done at large scale of the entire urban system. The relation between the distribution of amenities within the city and its spatial pattern is also discussed.

Introduction

Study of urban systems—how they form and develop—constitutes an important portion of human knowledge, not only because it is about our own physical space of daily living but also for understanding the underlying mechanisms of human settlement and civilisation on the Earth's surface that may be fundamentally similar to other forms of organisation like biological cells in our body or animal colonies. Urban systems, or "cities" in modern terms, are typical example of highly complex systems[1–7] in which overwhelmingly many agents are interacting in non-trivial and non-linear manners over a wide spectrum of spatial and temporal scales. The results of such tangled interactions are the emergence of unexpected global patterns that cannot be solely derived from the local knowledge of individual agents. Among these complex patterns are the spatial patterns delineated by the physical locations and shapes of urban entities like buildings, parks, lakes or infrastructure *etc.*..., *i.e.* the urban morphology.[8] A good understanding of the morphology of an urban system provides us with the comprehension of its current status of development or even the living condition of people inside it. For example, the number of residential buildings is a good gauge of the population size and the population density measures the crowdness that every resident has to experience in his or her daily life, or the infrastructure is an indicator of how well the city is doing in terms of economy.

In the recent years, with the availability of technologies and new mapping techniques, various forms of data on urban systems have been collected.[9] These data sets have enabled researchers to gain a deeper insight into the spatial structures existing in urban systems. One such data set is on the street and road networks which form the backbone of any urban system, and therefore, contain rich information about how the city is organised. A good amount of research have been performed on understanding the pattern of streets in many different cities around the world.[10–16] However, there are shortcomings of studying urban morphology based on street network when it has been noticed that the streets are not always well defined.[16,17] Public transport points, conversely, are well defined and can gauge the level of socio-technical development in an urban system as they represent the degree of mobility activities taking place within the urban system. Furthermore, public transport network is design to serve the residents of the city to perform activies on every aspect of daily life (going to school, commuting to work, shopping, entertainmment *etc.*...), and therefore, can be used as a good proxy of the residential distribution within a city. At the interplay of these factors, spatial pattern of distribution of transport points can provide us with rich insights into the morphology or, in some cases, even the morphogenesis of an urban system.

In this study, we will explore the spatial patterns encompassed in urban systems by analysing the pattern of spatial distribution of transport points (bus stops) in their public transport network of 73 cities around the world (see "**Data**").

---

[*]https://sites.google.com/site/nelive/
[†]http://www.baseride.com/
[‡]http://www.erikalegara.net/
[§]http://www.chrismonterola.net/
[¶]http://www3.ntu.edu.sg/home/lockyue/

The analysis shall reveal that there exists a typical value of distance among transport points within each city. This characteristic distance reflects the accessibility of each transport point and connectivity of them as an entire network, and hence, can be employed in measuring the physical area of the transport network's coverage. Interestingly, this area is shown to exhibit a scaling relation against the characteristic distance with a non-trivial value of the scaling exponent. Furthermore, the spatial distribution pattern of the transport points can be quantified and shown to belong to two main groups in which the points are either approximately equidistant or they are distributed apart with multiple length scales. The first group contains cities that appear to be well-planned, *i.e.* organised type, while the second consists of cities that tend to spread themselves over a large area and possess non-uniform spatial density of urban entities at different length scales, *i.e.* organic type. In addition to public transport network, we also look at the distribution of amenities within each city to investigate the relation between these two types of urban entity. We first find that the distance between amenities to their nearest transport points within a city follows a robust exponential distribution across all the cities considered, regardless of the city's type being organised or organic. Subsequently, we observe a clear quantifiable relation between this amenity-transport point distance and the density of transport points; and the type of the city can also be seen in this relation.

Results

Using a method of cluster analysis inspired by percolation theory,[18] we are able to characterise the spatial pattern of public transport points in urban systems. The spatial spattern is characterised by quantifying the size and area of a dominant cluster of transport points as functions of a distance parameter. This distance parameter (also the buffer radius) ρ represents the extent of vicinity around every transport point in the system, hence, the point's connectivity. Larger value of ρ means the neighbourhood of a point is extended, and therefore, can encompass more points within it. A pair of points are said to belong to the same cluster if and only if the Euclidean distance between them is less than or equal to ρ. The size of a cluster is defined as the number of points in the cluster while its area the union of area of circles of uniform radius ρ centred at the points in the cluster. A dominant cluster is the cluster with either largest size $\xi_{max}(\rho)$ or largest area $A_{max}(\rho)$. The clusters in the two occasions are not necessarily the same one. For simplicity of all discussions below, unless stated explicitly, descriptions for cluster size ξ also hold for cluster area A.

When ρ is small, the number of clusters $\eta(\rho)$ is large because most of the points are not connected and they form their own clusters. As ρ increases, $\eta(\rho)$ decreases monotonically because of merger of small clusters. In fact, it is a step function because the pairwise distances between points are discrete in value. On the other hand,

the size of the largest cluster $\xi_{max}(\rho)$ increases monotonically as ρ increases. Again, it is also a step function, but we assume in this study that the profiles $\xi_{max}(\rho)$ and $A_{max}(\rho)$ can be approximated by well behaved and smooth functions so that their derivatives exist at all points (see "**Characteristic distances among transport points**" and "**Spatial patterns in urban systems**"). In the regime of small buffer radius ρ, $\xi_{max}(\rho)$ slowly increases because the clusters are still disjoint. As ρ enters an intermediate regime, $\xi_{max}(\rho)$ increases faster than it does in the small-ρ regime. This is when the larger clusters merge together making the significant expansion in size of the largest cluster. As ρ increases further, there is no further significant change to the size of the largest cluster as it has encompassed most of the points in the domains, leaving only minor portions surrounding. The intermediate regime of ρ, therefore, could be seen as a region of "phase transition", similar to that in physics,[19] particularly percolation.[18]

In percolation, every point is assigned a variable called the percolating probability that controls the ability of one site to connect to another in the domain. The higher the percolating probability is, the easier the site is connected to others, and *vice versa*. The percolating probability is then viewed as a control parameter in the system. The transition occurs when the control parameter is adjusted to a critical value (called the critical point) at which the system transits from one state (or phase) to another with distinct properties, namely the non-percolating and percolating phases respectively at low and high percolating probabilities. The behaviours of the system approaching the critical point can then be used to classify the system, *i.e.* identifying its universality class.[20]

Applying this idea to our system of transport points within a city, the buffer radius ρ could be viewed as the control parameter. For small values of ρ, the system is in *segregate* phase, while it is in *aggregate* phase for large values of ρ. The transition from one phase to the other takes place in the intermediate regime of ρ. The manner in which the profiles of the largest system size $\xi_{max}(\rho)$ and area $A_{max}(\rho)$ transit through this region can characterise how the transport points are distributed within a city.

Characteristic distances among transport points

The intermediate regime of ρ can be identified and characterised by analysing the first derivative $\xi'_{max}(\rho) = \dfrac{d\xi_{max}(\rho)}{d\rho}$ of the cluster size. This quantity, which is interpreted as the rate of cluster size growth per unit of buffer radius, produces a peak every time a jump occurs in the cluster size $\xi_{max}(\rho)$, *i.e.* when the cluster merges with others and grows. Every peak in $\xi'_{max}(\rho)$, therefore, signifies the existence of one or a few clusters of points located at a farther distance beyond those in the current largest cluster that is being traced. As a result, this would provide us with the information on the length scales of distribution of points within the set. It can be easily seen that if there are many peaks, the points are distributed in clusters that are apart with different distances; whereas the ex-

istence of few peaks implies a uniform distribution of points that are (approximately) equidistant from one another. In either case, it is without doubt that there exists a characteristic distance in the spatial distribution of points. This characteristic distance should tell us the length scale above which the points are (largely) connected and below which they are disconnected.

Since all peaks in the derivative $\xi'_{max}(\rho)$ contribute to the growth of the cluster $\xi_{max}(\rho)$, a measure of the characteristic distance $\rho_\xi^\star$ must take into account the effects of all of them. However, a high peak indicates a more significant increase in cluster size (a major merger) than that indicated by a lower one. Hence, the average of all values of $\rho_{\xi,i}^\dagger$ at which a peak i occurs, weighted by the height $\xi'_{max}(\rho_{\xi,i}^\dagger) = \dfrac{\mathrm{d}\xi_{max}(\rho)}{\mathrm{d}\rho}\bigg|_{\rho=\rho_{\xi,i}^\dagger}$ of the peaks, is an appropriate measure of this characteristic distance, *i.e.*

$$\rho_\xi^\star = \frac{\sum_i \xi'_{max}(\rho_{\xi,i}^\dagger)\rho_{\xi,i}^\dagger}{\sum_i \xi'_{max}(\rho_{\xi,i}^\dagger)}. \tag{1}$$

Similarly, we have for the cluster area

$$\rho_A^\star = \frac{\sum_i A'_{max}(\rho_{A,i}^\dagger)\rho_{A,i}^\dagger}{\sum_i A'_{max}(\rho_{A,i}^\dagger)}. \tag{2}$$

The analyses of peaks in size profile $\xi'_{max}(\rho)$ and area profile $A'_{max}(\rho)$ provide different perspectives on the spatial distribution of points. The size quantifies the number of points with respect to the distance while the area further takes into account the relative position of the points. The two are not redundant but rather, one is complementary to the other. This comes to light in the next section "**Spatial patterns in urban systems**" when the combination of the two allows us to classify distinct types of distribution of points.

It is noteworthy that $\rho_\xi^\star$ and $\rho_A^\star$ are different from the average of pairwise distance among all points in the set because they encode the connectivity of the points in terms of spatial distribution. In other words, the two characteristic distances are measure of typical distance between points in the set in the perspective of global connectivity of all points. In the context of transport points, they translate to the distance one has to traverse to get from one point to another in order to explore the entire system. It then follows that a large value of characteristic distance implies a sparsely distributed set of points which could reflect a poorly covering network of transport. This agrees with a low density of points per unit area (see "**Area of system of transport points**" for more details). For the 73 cities considered in this study, $\rho_\xi^\star$ is found to be in the range $200-1200$m with most cities having $\rho_\xi^\star$ in the range $200-500$m. The ranges are $200-1700$m and $300-500$m for $\rho_A^\star$.

Spatial patterns in urban systems
The characteristic distances introduced above tell us whereabout the transitions of cluster size and area take place but they do not tell us how the size and area of the cluster transit from small to large value, *i.e.* how the cluster grows. This, however, can be easily characterised by further exploiting the analysis of peaks in $\xi'_{max}(\rho)$ (and $A'_{max}(\rho)$). It is a matter of fact that if the cluster grows rapidly through the transition, there are very few peaks in $\xi'_{max}(\rho)$, all of which are sharp and localised. On the other hand, the peaks are scattered over a wide range of ρ should the cluster gradually grow. The standard deviation of the location $\rho_{\xi,i}^\dagger$ of the peaks, or the spread of transition σ_ξ for cluster size, is a good measure of such scattering. However, a low peak that is distant from a group of localised high peaks should not significantly enlarge the spread. Therefore, the standard deviation of $\rho_{\xi,i}^\dagger$ needs to be weighted by the height $\xi'_{max}(\rho_{\xi,i}^\dagger)$ of the peaks, *i.e.*

$$\sigma_\xi = \sqrt{\frac{\sum_i \xi'_{max}(\rho_{\xi,i}^\dagger)\left(\rho_{\xi,i}^\dagger - \rho_\xi^\star\right)^2}{\sum_i \xi'_{max}(\rho_{\xi,i}^\dagger)}}. \tag{3}$$

Similarly, we have the spread of transition for cluster area

$$\sigma_A = \sqrt{\frac{\sum_i A'_{max}(\rho_{A,i}^\dagger)\left(\rho_{A,i}^\dagger - \rho_A^\star\right)^2}{\sum_i A'_{max}(\rho_{A,i}^\dagger)}}. \tag{4}$$

The combination of these two spreads of transition enables us to characterise the pattern of different types of spatial point distribution by interpreting different regions of the (σ_ξ, σ_A) diagram (see Fig. 1). There are four different types of distribution that can be identified using the spreads of transition in size σ_ξ and area σ_A. The first one is the region of small $\sigma_\xi \approx \sigma_A$ in which both $\xi_{max}(\rho)$ and $A_{max}(\rho)$ exhibit a sharp rise. The second one is the stripe of medium-to-large $\sigma_\xi \approx \sigma_A$ in which $\xi_{max}(\rho)$ and $A_{max}(\rho)$ exhibit gradual increase and almost every peak in $\xi'_{max}(\rho)$ has a respective peak in $A'_{max}(\rho)$. The third one is the region of $\sigma_\xi \gg \sigma_A$ in which the peaks in $\xi'_{max}(\rho)$ tend to spread over a wider range of ρ than those in $A'_{max}(\rho)$. The last one is the region of $\sigma_\xi \ll \sigma_A$ in which the peaks in $\xi'_{max}(\rho)$ tend to be more localised than those in $A'_{max}(\rho)$.

In this analysis, for practical purpose, the regions are determined by a 50-meter rule. According to that rule, $\sigma_\xi, \sigma_A < 50$ constitute the small $\sigma_\xi \approx \sigma_A$ region, $\left|\sigma_\xi - \sigma_A\right| < 50$ $(\sigma_\xi, \sigma_A > 50)$ constitute the medium-to-large $\sigma_\xi \approx \sigma_A$ region, $\sigma_\xi - \sigma_A > 50$ constitute the $\sigma_\xi \gg \sigma_A$ region and $\sigma_\xi - \sigma_A < 50$ constitute the $\sigma_\xi \ll \sigma_A$ region.

Single-scale regular pattern
In the bottom left corner of the (σ_ξ, σ_A) plot lie the points with $\sigma_\xi, \sigma_A < 50$. These points represent the profiles of $\xi_{max}(\rho)$ and $A_{max}(\rho)$ with localised peaks in both $\xi'_{max}(\rho)$ and $A'_{max}(\rho)$. This signifies a characteristic length scale at
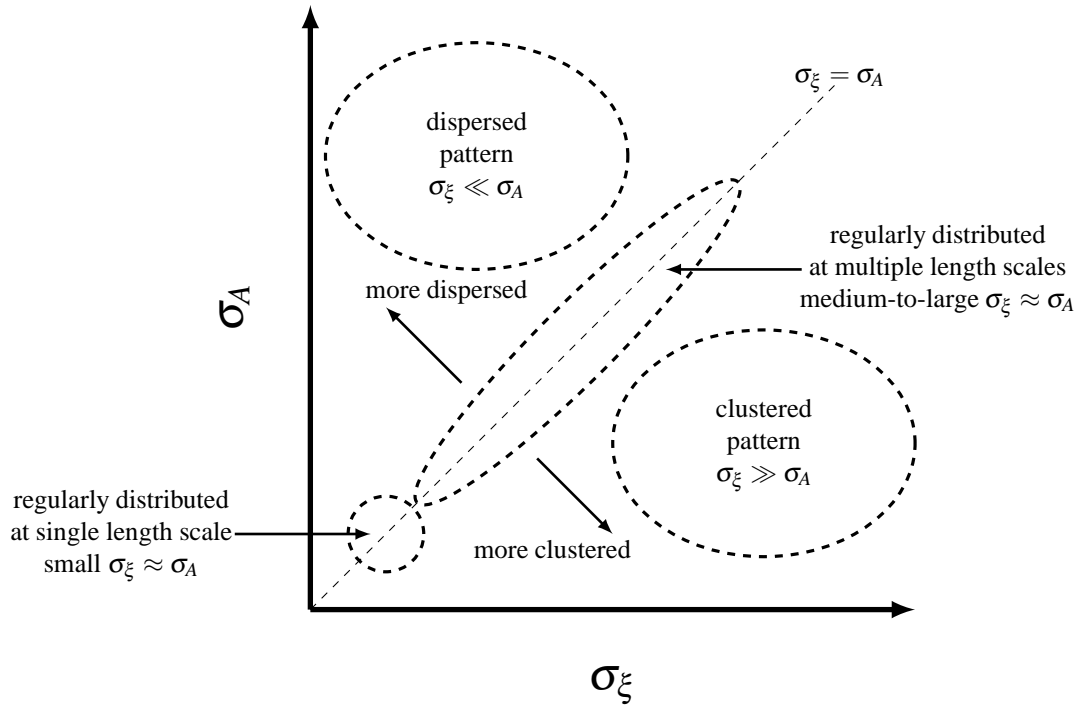
Figure 1. Interpretation of different patterns of spatial point distributions given different values of the pair (σ_ξ, σ_A).

which most of the points are (approximately) equally spaced from each other, *e.g.* grid points. The boroughs of Bronx, Brooklyn and Manhattan of New York city are typical examples of such kind of distribution (see Fig. 3(a)). The spatial pattern of the transport point in these cities appears very regular. In fact, inspecting their street patterns, one can easily tell the pattern of parallel roads in one direction cutting those in the other dividing the land into well organised polygons with almost perfect square and rectangular shapes. Apparently, this feature must be a result of well-designed and top-down planning before actually building the infrastructure in the city.[13]

***Multiple-scale regular pattern***
The transport points in a city can also be distributed in a regular manner but at different length scales. For example, the entire set of points can be divided into several subsets and within each subset, the points are (quasi-)equally distant from each others. At larger length scale, *i.e.* ρ increases further, these subsets of points are again (quasi-)equally distant from each other, *i.e.* hierarchical structure. The buffer radius ρ can thus be thought to play the rôle of a zooming parameter. In this multi-scale regular pattern, the profile of the largest cluster size $\xi_{max}(\rho)$ and area $A_{max}(\rho)$ experience a significant jump every time ρ changes its zooming level. At the lowest level are individual transport point. When ρ zooms out to the second level, the points that are closest to each other start to form their respective clusters. Moving to the next level, the nearby clusters start joining to form larger cluster but there will be many of these "larger clusters", *i.e.* the

largest cluster is of comparable size or area to several other clusters. The most important feature of this spatial pattern is that the jumps in the profile of $\xi_{max}(\rho)$ correspond well to those in $A_{max}(\rho)$, even though the locations of the jumps are spread apart. That leads to the (approximate) equality of the spread of transitions σ_ξ and σ_A despite their not being small. A good example of this type of distribution is the city of Epsom in Auckland, New Zealand (see Fig. 3(b)).

It is also interesting to note that within a city itself, different parts can possess distinct spatial patterns of the transport points. For example, even though New York city is known to be a well-planned city with grid-like street patterns, not all of its five boroughs share that nice feature. Only Manhattan, Bronx and Brooklyn have small σ_ξ and σ_A while the spreads are larger for the other two boroughs, Queens and Staten Island. This fact indeed complements the result reported earlier that Queens exhibits a distinct spatial pattern different from the other boroughs.[16] St Louis in Missouri, USA, is another interesting example. Two halves of the city on the two banks of Mississippi river appear to have different spatial patterns when they possess different values of the pair σ_ξ and σ_A.

Clustered pattern
There are cases in which the jumps in the profile of largest cluster size $\xi_{max}(\rho)$ don't correspond to those in the area $A_{max}(\rho)$ and *vice versa*. In such cases, the spatial distribution of the transport points deviates from regular patterns. We first consider the scenarios in which $\sigma_\xi \gg \sigma_A$. For such distributions, the points are clustered and tend to minimise the coverage area. When $\sigma_\xi \gg \sigma_A$, there are jumps in the size
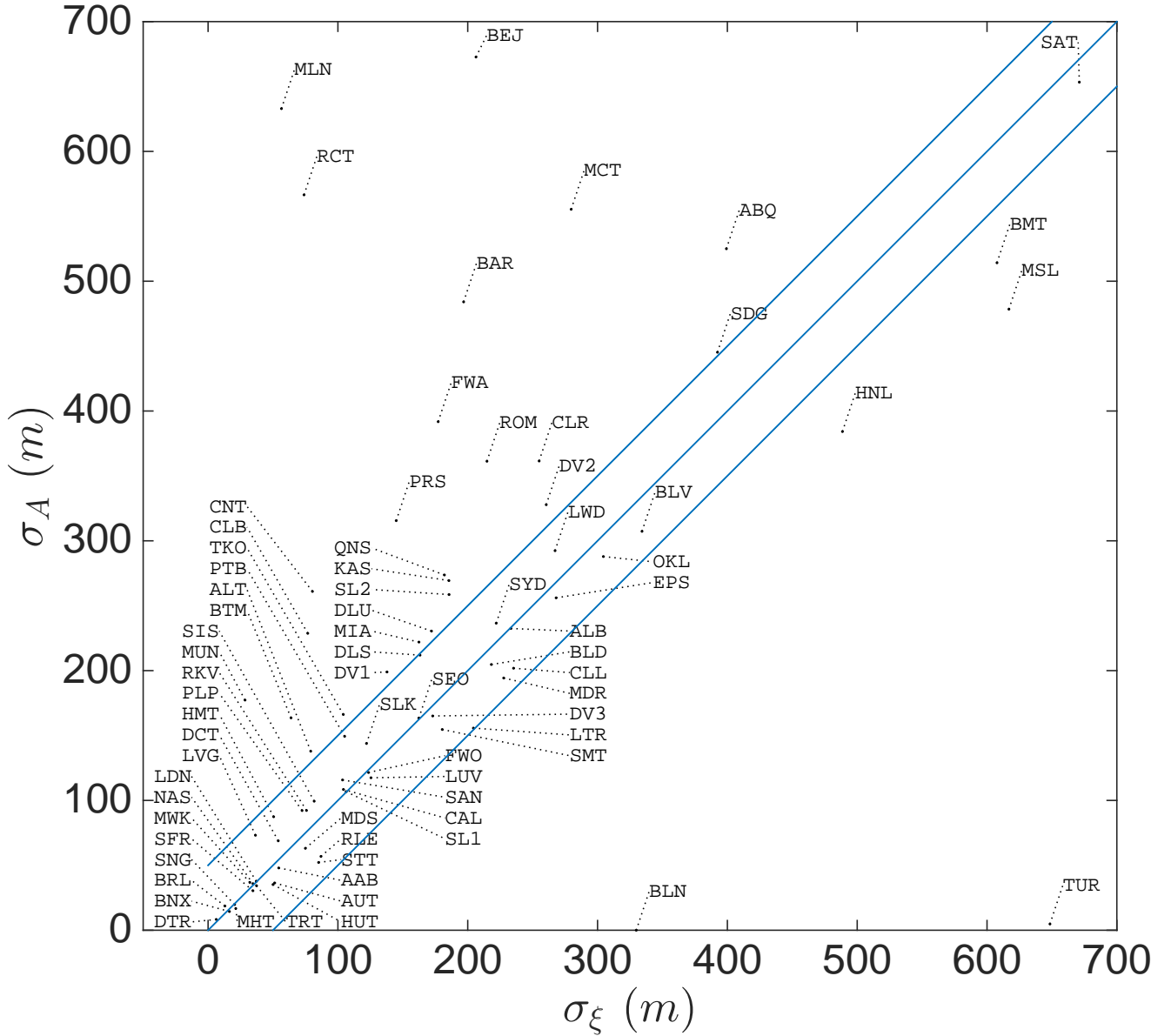
| AAB: Ann Arbor (US)	BTM: Baltimore (US)	EPS: Epsom (NZ)	MDR: Madrid (ES)	QNS: Queens (US)	SLK: Salt Lake City (US)
ABQ: Albuquerque (US)	CAL: Calgary (CA)	FWA: Fort Wayne (US)	MDS: Madison (US)	RCT: Rochester (US)	SMT: Sacramento (US)
ALB: Albany (US)	CLB: Columbus (US)	FWO: Fort Worth (US)	MHT: Manhattan (US)	RKV: Rockville (US)	SNG: Singapore (SG)
ALT: Atlanta (US)	CLL: Cleveland (US)	HMT: Hamilton (CA)	MIA: Miami (US)	RLE: Raleigh (US)	STT: Stockton (US)
AUT: Austin (US)	CLR: Colorado Springs (US)	HNL: Honolulu (US)	MLN: Milan (IT)	ROM: Rome (IT)	SYD: Sydney (AU)
BAR: Barcelona (ES)	CNT: Cincinnati (US)	HUT: Houston (US)	MSL: Marseille (FR)	SAN: Santa Ana (US)	TKO: Tokyo (JP)
BEJ: Beijing (CN)	DCT: Decatur (US)	KAS: Kansas City (US)	MUN: Munich (DE)	SAT: San Antonio (US)	TRT: Toronto (CA)
BLD: Boulder (US)	DLS: Dallas (US)	LDN: London (UK)	MWK: Milwaukee (US)	SDG: San Diego (US)	TUR: Turin (IT)
BLN: Berlin (DE)	DLU: Duluth (US)	LTR: Little Rock (US)	NAS: Nassau County (US)	SEO: Seoul (KR)	
BLV: Belleville (US)	DTR: Detroit (US)	LUV: Louisville (US)	OKL: Oakland (US)	SFR: San Francisco (US)	
BMT: Bremerton (US)	DV1: Denver 1 (US)	LVG: Las Vegas (US)	PLP: Pinellas Park (US)	SIS: Staten Island (US)	
BNX: Bronx (US)	DV2: Denver 2 (US)	LWD: Lakewood (US)	PRS: Paris (FR)	SL1: St Louis 1 (US)	
BRL: Brooklyn (US)	DV3: Denver 3 (US)	MCT: Manchester (UK)	PTB: Pittsburg (US)	SL2: St Louis 2 (US)	

Figure 2. Types of spatial distribution of transport points in cities across the globe. The three reference lines are $\sigma_A = \sigma_\xi$, $\sigma_A = \sigma_\xi + 50$ and $\sigma_A = \sigma_\xi - 50$.

of the largest cluster size that do not give rise to a jump in its area. This happens when the points of an acquired cluster are compact, contributing very little increase in the area of the largest cluster. If the acquired cluster are not compact, *i.e.* its points span a larger area, there might be significant increase in the area of the largest cluster and, hence, a peak would be
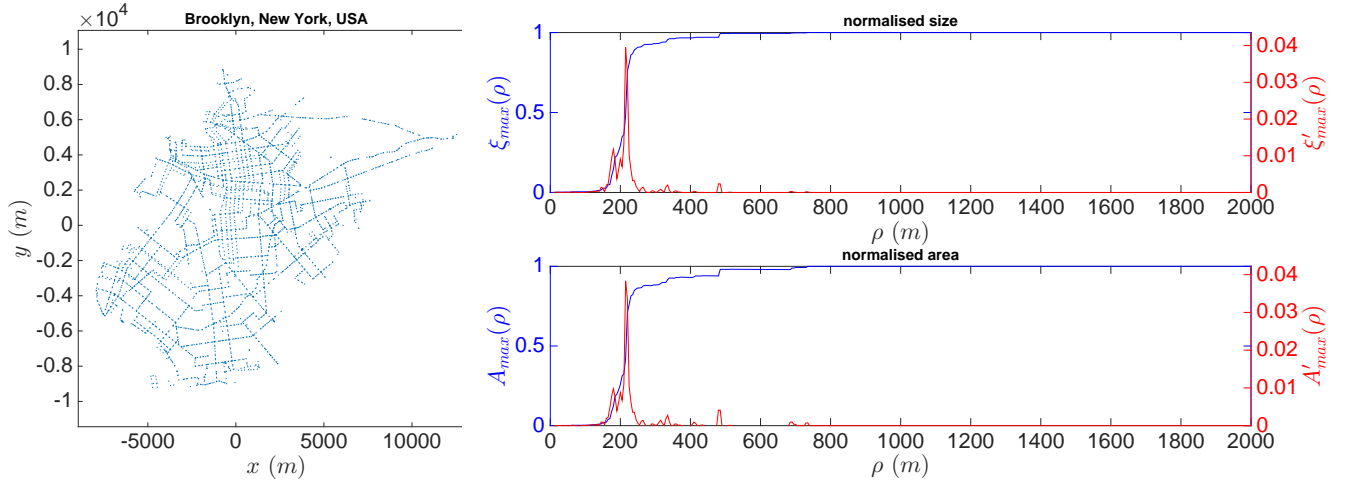
(a) Brooklyn, New York, USA. The spreads of transition for the size σ_ξ and area σ_A are both small. This is an example of single-scale regularly distributed pattern, *i.e.* grid.
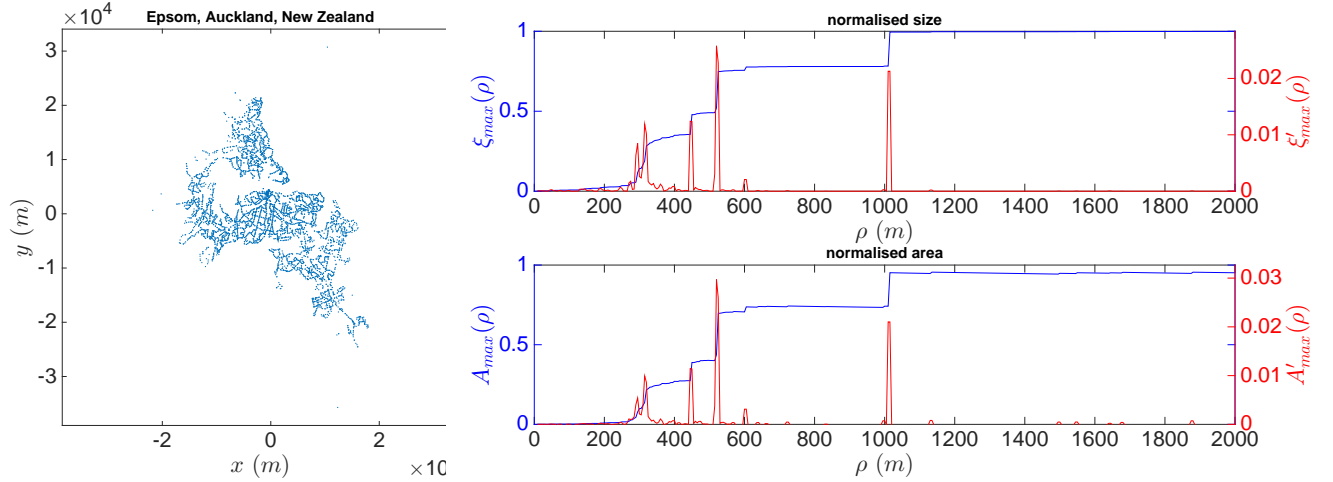
(b) Epsom, Auckland, New Zealand. The spreads of transition for the size σ_ξ and area σ_A are not small but stay comparable to one another. This is an example of multi-scale regularly distributed pattern.

Figure 3. Typical cities of single and multiple-scale regular spatial patterns. In each subfigure, the left panel shows the location of transport points within the city, the upper right panel the profile of largest cluster size $\xi_{max}(\rho)$ together with its first derivative $\xi'_{max}(\rho)$ and the lower right panel the profile of largest cluster area $A_{max}(\rho)$ together with its first derivative $A'_{max}(\rho)$

reflected by its contribution to σ_A. However, the size measure is not affected as it only tells the number of points that are included in the cluster but not their relative location with respect to each other.

The distribution of transport points in the city of Turin in Piedmont, Italy (see Fig. 4(a)), is a good example of this type. The points appear clustered and compactly distributed but not regular or grid-like.
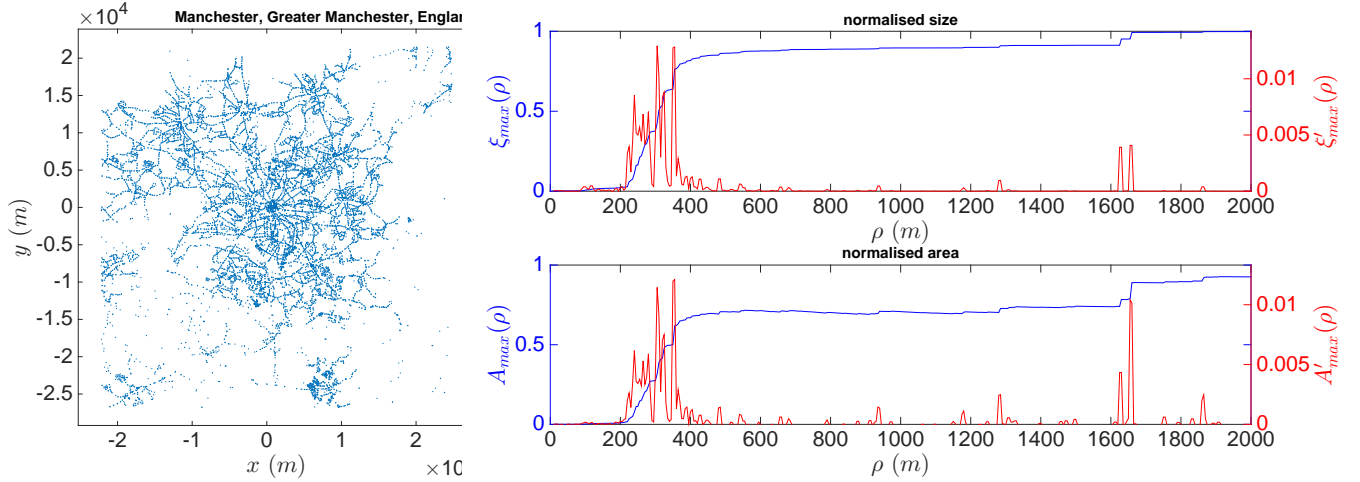
Dispersed pattern

On the other side, we have the scenarios of $\sigma_\xi \ll \sigma_A$, in which the points are dispersed and tend to maximise the coverage area. When $\sigma_\xi \ll \sigma_A$, there are jumps in the area of the largest cluster that do not give rise to a jump in its size.

This happens when the points of an acquired cluster are dispersed (but still within the buffer radius so that they belong to the same cluster). This way, the increase in the area of the largest cluster is more significant than that in its size, resulting $\sigma_\xi \ll \sigma_A$. A good example of this type is the distribution of transport points in Manchester in Greater Manchester, England (see Fig. 4(b)). The points appear in dispersed pattern of long roads around the city.

If the feature of single-scale regular spatial pattern (when both σ_ξ and σ_A are small) is a result of well-designed and top-down planning in an urban system, the other spatial patterns (either σ_ξ or σ_A is not small) can be intepreted as a consequence of developing an urban system under local constraints. In the former case, the urban system appears to be
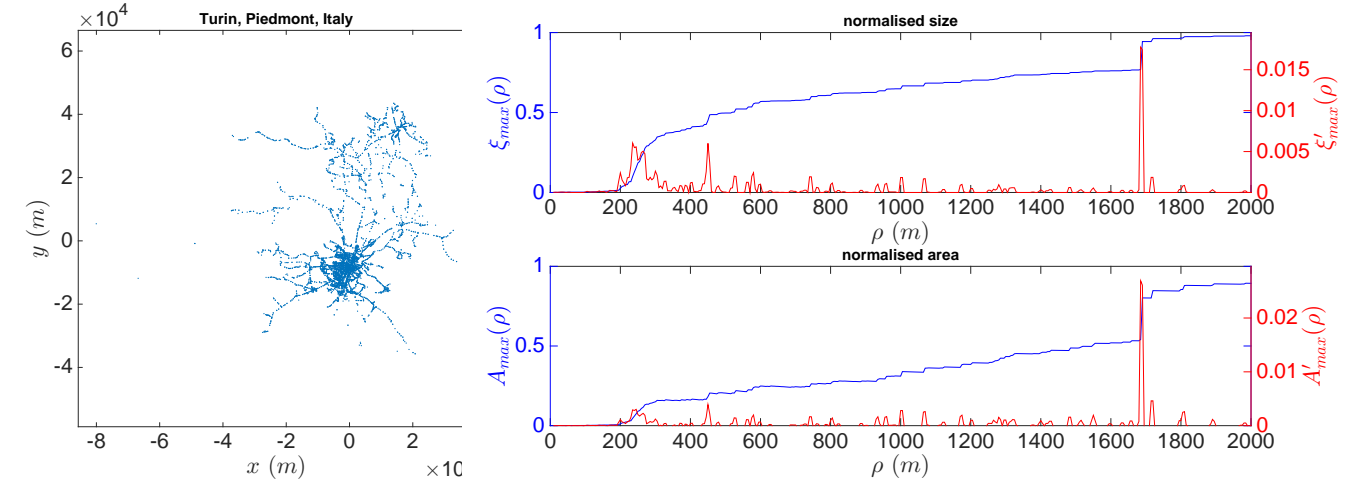
(a) Turin, Piedmont, Italy. The spread of transition in peaks for the size is more than that for the area of the largest cluster, $\sigma_\xi > \sigma_A$. This is an example of clustered pattern.

(b) Manchester, Greater Manchester, England. The spread of transition in the peaks for the size is less than that for the area of the largest cluster, $\sigma_\xi < \sigma_A$. This is an example of dispersed pattern.

Figure 4. Typical cities of clustered and dispersed spatial patterns. In each subfigure, the left panel shows the location of transport points within the city, the upper right panel the profile of largest cluster size $\xi_{max}(\rho)$ together with its first derivative $\xi'_{max}(\rho)$ and the lower right panel the profile of largest cluster area $A_{max}(\rho)$ together with its first derivative $A'_{max}(\rho)$

of organised type while in the latter, it can be said to be of organic type when its spatial features develop in an adhoc manner as the city grows. The revelation of spatial patterns in urban systems from the analysis in this work could imply two different types of process that the cities undergo through their course of development.

Visually inspecting the spatial distribution of transport points within the cities, it appears that cities with regularly distributed pattern, either single- or multiple-scale, do not have an apparent centre. That means there is no spatial preference in the distribution of the points, *i.e.* no part is special than the others. This is in contrast to the other two types of cities in which star-node structure can be clearly observed. The node represents the centre of the city at which there is higher density of transport points than the other areas, and

from which the roads diverge radially to the outer part of the city. This observation could by explained by the growth process of different types of urban system. When a city grows organically, it starts from a central business district and gradually expands to encompass the nearby area to accommodate more people wanting to participate the business activities at the centre. On the other hand, when a city is planned before, the planners seem not to concentrate the infrastructure in one confined area but stretch it across the entire city.

Universal features in urban systems
Area of system of transport points
Despite the difference in the spatial pattern of the distribution of transport points, all the cities considered in this study appear to possess a common relation between the density of

points and the characteristic distance of area $\rho_A^\star$. To explore this, we first define the characteristic area of a set of points which is the union area of circles of radius $\rho_A^\star$ centred at all points in the set, $\Xi(\rho_A^\star)$. The characteristic distance of area $\rho_A^\star$ represents the typical value of ρ at which the area of the entire system experiences the transition. Further increase in ρ after that does not contribute to as much increase in the area of the largest cluster and the cluster, thus, would entail unnecessary area. The value of $\Xi(\rho_A^\star)$ is therefore expected to be a good proxy to the essential area covered by the set of points given their spatial distribution. In the case of transport system, we call this area the serving area of all the transport points.

Having defined the area, it is easy to calculate the density of points per unit area, which is simply the ratio between the number of points and the area they cover, $\dfrac{N}{\Xi(\rho_A^\star)}$. From empirical analysis, we find the data fit very well to the relation

$$\frac{N}{\Xi(\rho_A^\star)} \propto (\rho_A^\star)^{-\tau} \tag{5}$$

with $\tau \approx 1.29$. Figure 5 shows the empirical relation between the two quantities. The relation in Eq. (5) is well obeyed by all 73 cities. It is a remarkable relation given the scattered relation between $\rho_A^\star$ and N or $\Xi(\rho_A^\star)$. For reference, the artificial generated data, including both random and regular patterns (see "**Discussion**" for details) are also included in the plot but not in the fitting itself. As can be observed, those points generally stay below the points for the 73 cities.

It should be further noted that the relation in Eq. (5) or Fig. 5 is not a trivial one. To see this, we consider the two scenarios of ρ in extreme limits, $\rho \gg 1$ and $\rho \ll 1$, and its relation with $\dfrac{N}{\Xi(\rho)}$. For the small extreme value, $\rho \ll 1$, all clusters include only a single point, and there are, hence, N clusters. We, therefore, have

$$\Xi(\rho) = N\pi\rho^2 \tag{6}$$

which yields the relation

$$\frac{N}{\Xi(\rho)} = \frac{1}{\pi\rho^2} \propto \rho^{-2}. \tag{7}$$

At the other extreme value, $\rho \gg 1$, there is only one single cluster that encompasses all points concentrating at the centre of the union area. We, therefore, have

$$\Xi(\rho) \approx \pi\rho^2, \tag{8}$$

which leads to

$$\frac{N}{\Xi(\rho)} \approx \frac{N}{\pi\rho^2}, \tag{9}$$

which in turn displays scaling behaviour like in Eq. (5) if and only if the number of points N scales with ρ.

The whole argument about the extreme values of ρ is to illustrate that the scaling relation in Eq. (5) with exponent

$\tau = -1.29$ is not a relation that can be achieved with any value of ρ. The relation can only hold at some value of the buffer radius like $\rho_A^\star$, given the structure in the distribution of N points. Because of this feature, we consider $\rho_A^\star$ *the* characteristic distance of a set of spatially distributed points.

Amenity distribution

Beside transport system, which is represented by a network of transport points, the morphology of an urban system can also be understood from another angle by examing the distribution of amenities within it. It turns out that despite possessing different types of distribution of transport points, the cities appear to share a common universal distribution of amenities. The analysis of locations of amenities in all the cities reveals that the (Euclidean) distance Ω_k of an amenity k to its nearest transport point follows a robust exponential distribution. That means the probability of finding an amenity with distance Ω to its nearest transport point decays exponentially with Ω, *i.e.* its probability density function is given by

$$P(\Omega) = \lambda e^{-\lambda\Omega}, \tag{10}$$

which renders its mean and standard deviation (*not variance*) equal

$$\langle\Omega\rangle = \sigma(\Omega) = \sqrt{\langle\Omega^2\rangle - \langle\Omega\rangle^2} = \frac{1}{\lambda}. \tag{11}$$

In Fig. 6, the mean $\langle\Omega\rangle$ and standard deviation $\sigma(\Omega)$ of shortest amenity-transport point distance for different cities are shown to stay close to the diagonal line $\sigma(\Omega) = \langle\Omega\rangle$. The exponential distribution of the distance Ω is strongly supported by further veriyfing that higher moments of the distribution $P(\Omega)$ fit well to

$$\langle\Omega^n\rangle = \frac{n!}{\lambda^n}, \tag{12}$$

up to fourth order, $n = 4$.

It has to be emphasized that the distribution of distance from amenities to their nearest transport points follows an exponential rather than a Poissonian one. That means the mean of such distance is (approximately) equal to its standard deviation rather than variance which holds for a Poisson distribution. The robust distribution of amenities across all city types has one important implication that the local growth process in urban systems appears to be independent of human intervention and larger scale of the entire system. That means planners can plan the large-scale growth process like transportation but the small-scale growth process like local business still takes place on its own. But it remains a significant question why the distribution is exponential, not any other form. In fact, exponential decay in spatial urban patterns has been long reported in literature.[21] Using this feature as a fact, a model has been constructed to successfully capture the morphology of urban systems.[22]
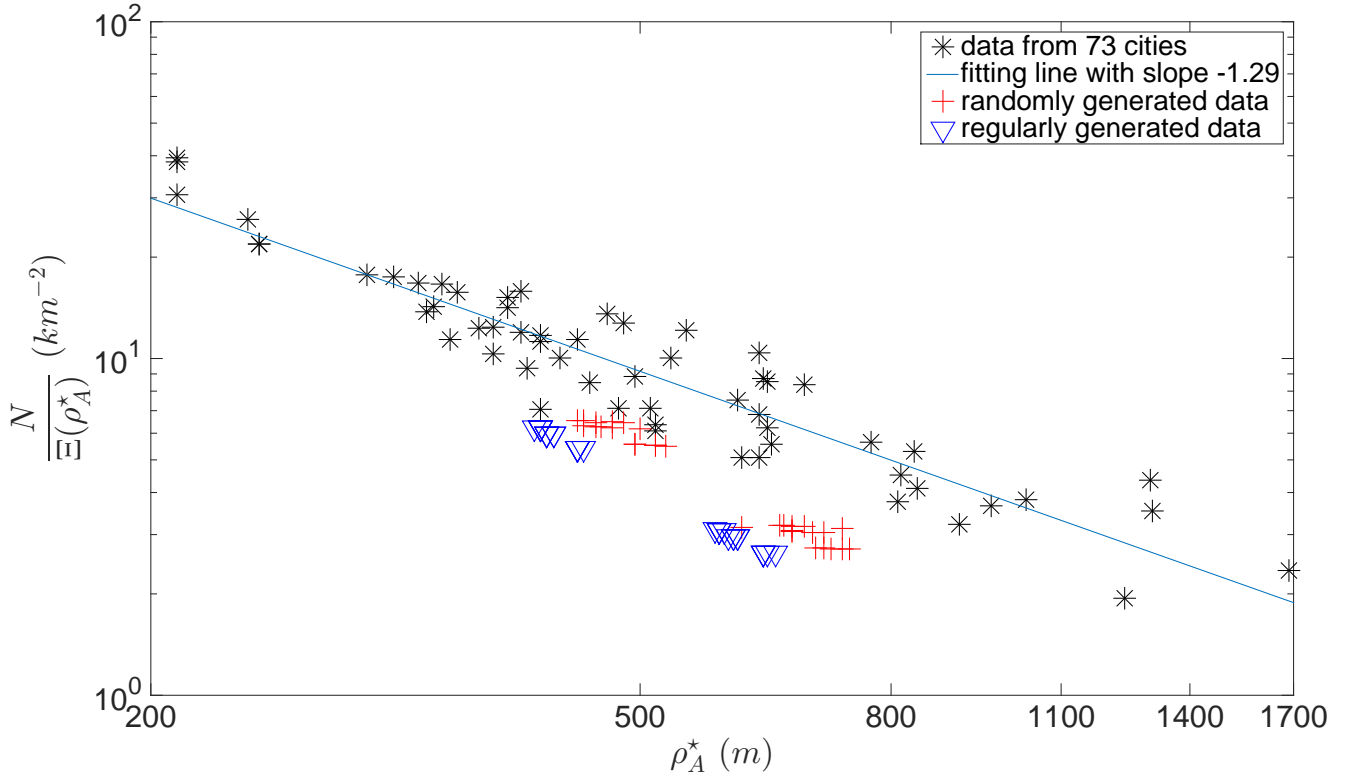
Figure 5. Empirical relation between density of point per unit area and the characteristic distance $\rho_A^\star$ in log-log scale. The fitting line has slope -1.29 and was obtained with linear regression coefficient of $R^2 \approx 0.8$. The artificial generated data, both random and regular, were not included in the fitting.

Relation between transport point and amenity distributions

There appears to be a relation between the density of transport points within a city and the distribution of its amenities. Figure 7 depicts this relation by plotting the average distance $\langle \Omega \rangle$ against the density $\dfrac{N}{\Xi(\rho_A^\star)}$. It could be observed that only the lower-left triangle of the plot is occupied, leaving no points in the upper-right corner of the plot. That means there are no cities with high density of transport points and, at the same time, having large (average) distance between its amenities and the nearest transport points. This can be easily understood by the fact that in cities with high density of the transport points, the road network is very dense, the transport points have to stay within a short distance of each other. As a result, the amenities must necessarily be built very close to the public transport points. It turns out that those cities with very high density of transport points are those with single-scale regular pattern of distribution, *i.e.* the points are regularly distributed at (approximately) equal distances from each other like grid points, such as San Francisco or the boroughs of New York city.

At the other end, the cities with low density of public transport points can exhibit a wide spectrum of average amenity-transport point distance $\langle \Omega \rangle$. These cities can either have large or small $\langle \Omega \rangle$. A large value of $\langle \Omega \rangle$ (and hence, large standard deviation $\sigma(\Omega)$, too) implies a city with sparse distribution of amenities when they are distant from the nearest transport point like Dallas or San Antonio in Texas, USA. On the other hand, a small value of $\langle \Omega \rangle$ suggests that the amenities are built close to public transport points implying the existence of sub-centres or several small towns or districts within the city, such as Turin in Piedmont, Italy.

Discussion

The present work analyses the features of the spatial distribution patterns of important entities in an urban system, the public transport points and the amenities. The former ones are part of the backbone of any urban system, the street network which plays essential rôle in enabling flow or exchange of various processes in the city. The advantage of knowledge of these transport points is that they can be well defined and easily collected and at the same time provide other information like the residential distribution within the city. The latter ones, on the other hands, can gauge the size of population as well as the level of activities in the city. The results unveil different types of city with distinct spatial patterns. The cities are shown to be either of organised type, in which the entities are well spaced as if they are built top-down, or of organic type, in which the entities are spaced with multiple length
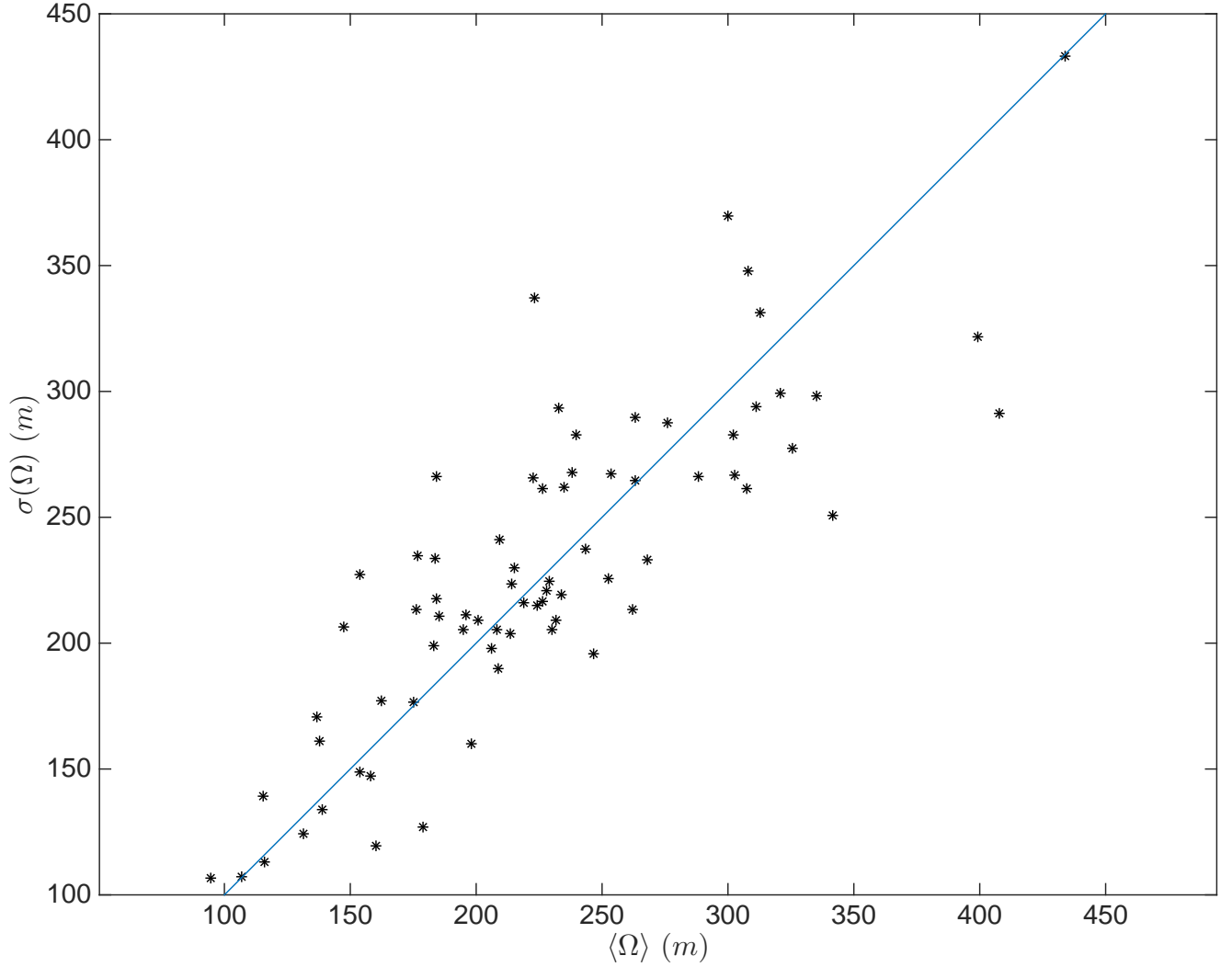
Figure 6. Standard deviation $\sigma(\Omega)$ *vs.* mean $\langle\Omega\rangle$ of distance from amenities to nearest transport points within each city. The reference line is $\sigma(\Omega) = \langle\Omega\rangle$.

scales as if they grow spontaneously. In either cases, the typical distance among the transport points can be described by a characteristic distance. Despite the different types of the cities' spatial patterns, the density of the transport points exhibits universal scaling behaviour with this characteristic distance. On the other hand, the distance from amenities to their nearest transport points also follows a robust exponential distribution for all cities studied. Furthermore, there is an apparent relation between the distributions of transport points and amenities within the cities. These facts signify some universal mechanisms underlying the growth and development that all cities have to undergo.

In an attempt to understand the processes that generate the spatial distribution patterns of the transport points, we artificially generate some distributions of points on a two-dimensional surface. In the first distribution, the points are generated at random locations within a domain with uniform probability. In the second distribution, starting from a regular grid of points in a square lattice, the points are randomly displaced by a small amount not more than a quarter of the lattice spacing. It turns out that both the randomly and regularly generated data produce simple behaviours through our analysis. In particular, the peaks in size and area generally coincide with each other and stay localised (the random sets tend to produce more peaks while the regular ones have only one peak as expected), and hence, both σ_ξ and σ_A are small indicating regular pattern of distribution. At this point, we would like to link the analysis with the idea of measure of complexity of a symbolic sequence.[23–25] The idea states that both regular and random (in the sense of a random number generator) sequences possess very low measure of complexity as their structures or patterns are simple and easy to be presented in terms of the so-called ε-machine.[23] Along that line, it could be argued that the patterns observed in the distributions of transport points from the real data of 73 cities around the world are more complex then those in the artifi-
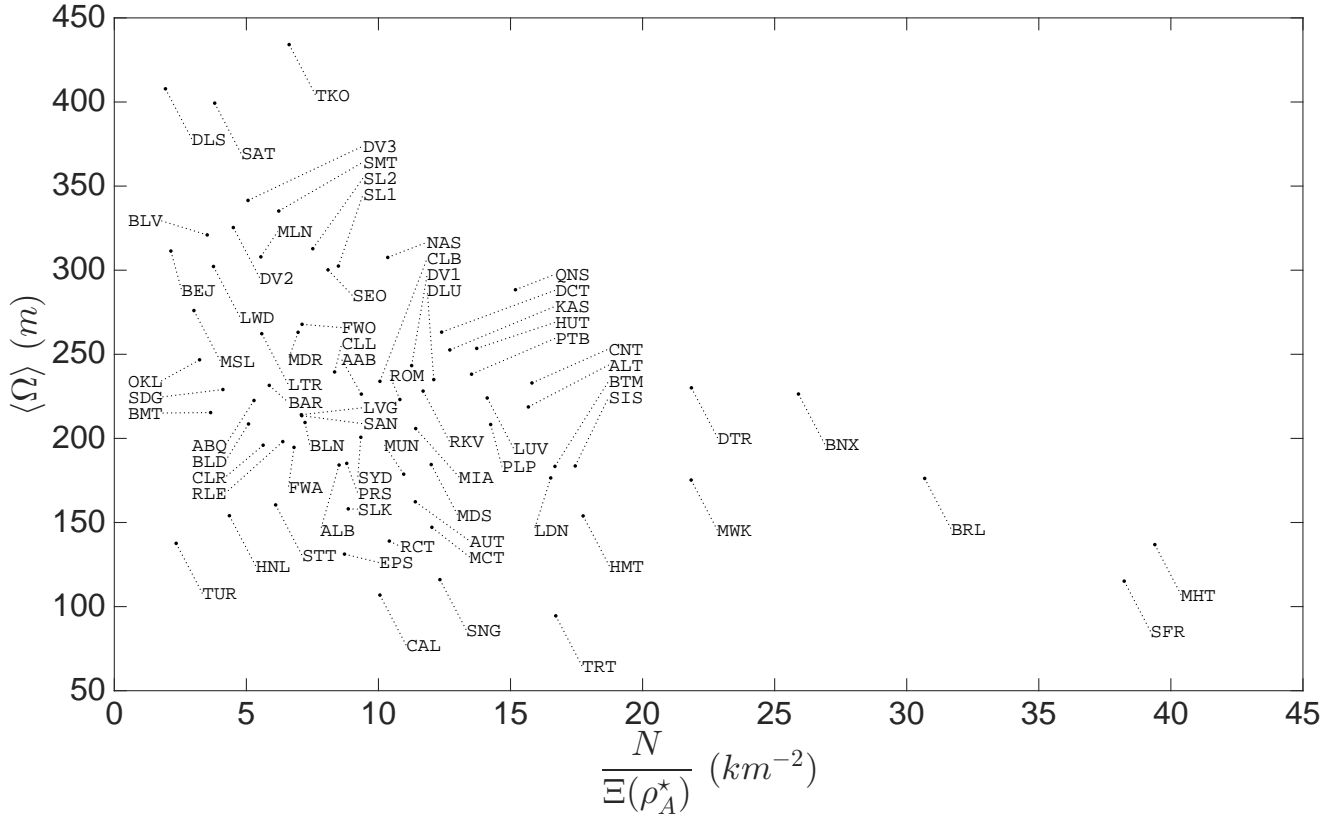
Figure 7. Relation between density of transport points $\frac{N}{\Xi(\rho_A^\star)}$ and average amenity-transport point distance $\langle \Omega \rangle$. Refer to Fig. 2 for codename of the cities.

cially generated data. The generated data, which is meant to be either regular or completely random possess, only simple structure as we have argued above with small spreads σ_ξ and σ_A. The real world data might well contain mixtures between regular and random patterns that could result in both the clustered and dispersed patterns that we have reported in "**Spatial patterns in urban systems**".

Method

General ideas

For the analysis, we propose a procedure to characterise the spatial pattern of a set of points. The procedure involves identifying clusters of points, whose pairwise distance does not exceed the value of a parameter, and quantifying the growth of the clusters as the parameter value increases.

Consider a domain $\mathfrak{D}$ which can be thought of as a city or a town. In this domain, there are N points i distributed, each of which represents a transport point located at coordinates (x_i, y_i). We introduce a parameter called the buffer radius ρ to construct the clusters. Any point j, whose distance

$$d_{ij} = \sqrt{(x_i - x_j)^2 + (y_i - y_j)^2} \qquad (13)$$

from point i is less than or equal to ρ, belongs to the same cluster as i. We denote $\eta(\rho)$ as the number of clusters given the buffer radius ρ. For each cluster α, we define the cluster size $\xi_\alpha(\rho)$ and the cluster area $A_\alpha(\rho)$. The cluster size is defined as the number of points in the cluster and the cluster area the union of area of circles of uniform radius ρ centred at the points in the cluster. To make different domains comparable, we normalise the cluster size $\xi_\alpha(\rho)$ by the number of points N in the domain, while the cluster area

$A_\alpha(\rho)$ by the union of area $\Xi(\rho)$ of circles of radius ρ centred at all points in the domain.

The identification of the clusters can be done by using a simple heuristic cluster finding algorithm that starts with a random points in the set and gradually identifies the other points of in the same cluster. Alternatively, one can employ the method of DBSCAN,[26] setting the noise parameter to be zero. The two methods are identical and yield the same results.

Analysis

For any cluster-related quantity, we attach the subscript ξ to associate it with cluster size while A for cluster area. For simplicity of all discussions, unless stated explicitly, descriptions for cluster size ξ also hold for cluster area A.

To quantify the spatial pattern of the set of points, we vary the buffer radius parameter ρ. As ρ increases, the farther points can belong to the same cluster. As a result, the clusters can merge to increase their size. Tracing the behaviour of the largest cluster $\xi_{max}(\rho)$ can provide us with the way the points are distributed within the set. For example, the profile of the first derivative $\xi'_{max}(\rho) = \frac{d\xi_{max}(\rho)}{d\rho}$ (and $A'_{max}(\rho) = \frac{dA_{max}(\rho)}{d\rho}$) can indicate at which distance ρ, the points are (largely) connected in a single cluster. Because $\xi_{max}(\rho)$ increases monotonically with ρ, we introduce the so-called *characteristic distance* $\rho_\xi^\star$ at which $\xi_{max}(\rho)$ exhibits the most significant increase. In some cases, the profile $\xi_{max}(\rho)$ shows a sharp narrow increase around a value ρ. While in other cases, several small increases are observed, spreading a wide range of ρ. To account for that, it is also meaningful to introduce a quantity σ_ξ, called *spread of transition*, to measure the overall width of the increases in the profile of ξ_{max}.

To recap, $\rho_\xi^\star$ is the value of ρ above which there is a significant transition in the largest cluster size $\xi_{max}(\rho)$ (see peak analysis in "**Peak analysis**"); σ_ξ measures the width of the transition. The respective quantities for cluster

area are $\rho_A^\star$ and σ_A. We then use the union area with this buffer radius $\rho_A^\star$ of all points in the system as the effective area $\Xi(\rho_A^\star)$ of the point set.

We refrain from looking at the average value of distribution of the cluster size or area as these measures are vulnerable against errors in data, *i.e.* outliers. For example, when the buffer radius ρ is sufficiently large that most but a few of the points in the dataset belong to a single large ("giant") cluster, there are only two (or more) clusters and the average cluster size would be half (or less) of what it is supposed to be.

Peak analysis

As the buffer radius ρ increases, the size of the largest cluster $\xi_{max}(\rho)$ also increases. It can be easily observed that the profile of $\xi_{max}(\rho)$ exhibits an either sharp or gradual increase. The former introduces a single dominant peaks in the profile of $\xi'_{max}(\rho)$ while the latter a set of peaks scattering over a wide range of ρ. This scattering of peaks can be quantified using the standard deviation of their locations, weighted by the strength (height) of the peaks. A small standard deviation implies a sharp increase in $\xi_{max}(\rho)$, and *vice versa*, a large standard deviation signifies a gradual increase.

In our analysis, we consider the profile of $\xi'_{max}(\rho)$ (and $A'_{max}(\rho)$) at every value of the buffer radius ρ ranging from $\rho_{min} = \rho_1 = 10$m to $\rho_{max} = \rho_M = 2000$m in the step of $\delta\rho = \rho_{i+1} - \rho_i = 5$m, $\forall i$. Since the values of the buffer radius are discrete, a point $(\rho_i, \xi'_{max}(\rho_i))$ is a peak if and only if

$$\begin{cases} \xi'_{max}(\rho_i) > \xi'_{max}(\rho_{i-1}) \\ \xi'_{max}(\rho_i) > \xi'_{max}(\rho_{i+1}) \end{cases}. \tag{14}$$

This discrete nature also produces a lot of small noisy peaks. In our analysis, we filter these noisy peaks by offsetting the entire profile of $\xi'_{max}(\rho)$ by a sufficiently small amount and considering only the positive remaining peaks.

The value of $\rho_\xi^\star$ will then be the mean of ρ of all peaks, weighted by the peak height $\xi'_{max}(\rho)$ (see Eq. (3)). The spread σ_ξ is the standard deviation of ρ of all peaks, again weighted by the peak height $\xi'_{max}(\rho)$ (see Eq. (4)).

Implementation

The cluster analysis is implemented in Python, using `shapely` library to calculate the union area. We also use `DBSCAN` library for DBSCAN analysis to compare with our method.

Data

Data collection

The public transit-related data was collected by Baseride Technologies using different available API (application programming interfaces) provided by transit agencies. Collected data included (but not limited to) GPS (global positional system) coordinates of bus stops, their characteristics (*e.g.* name), route geometry, bus stop sequence on the routes. Additional information was also collected for future analysis (schedules, trips, real time public transport location updates). Majority of agencies provides information through GTFS (general transit feed specification). Minority of cities are using their custommade APIs. Baseride converted all protocols into single uniform data representation. Information about public transit network was also converted into linked graph for convenient analysis using different methods. The data for Singapore was obtained from Transit Link Pte Ltd.[27] The data set was also augmented with data from OSM.

The amenity data for all cities was obtained from OSM through the Mapzen project.[28] An amenity is said not to belong the city if it is not within 1,000m of any bus stop in that city.

The datasets contain information about location of the bus stops in the form of latitude and longitude. The stops are grouped for the same city or municipal organisation. In the present analysis, we only select 73 cities with at least 1,000 bus stops. Those include the cities in England, France, Germany, Italy, Spain, Canada, United States, China, Japan, South Korea, Australia, New Zealand and Singapore. The full list of cities can be found in Fig. 2.

Data preprocessing

For each dataset, the spherical coordinates of each bus stop in latitude θ and longitude φ are transformed to quasi-planar two-dimensional Cartesian coordinates. We could have done the transformation by employing the Universal Transverse Mercator (UTM) conformal projection, but since all datasets are confined within areas on Earth's surface spanning less than 100km in both dimensions, we find the approximation method below sufficient, with errors being less than 0.5%.[29]

We convert the spherical coordinates $\boldsymbol{\phi}_i = (\varphi_i, \theta_i)$ to Cartesian coordinates $\boldsymbol{r}_i = (x_i, y_i)$ for every point i in the dataset by first setting the origin of the plot. The origin O is the centroid of all points

$$\boldsymbol{\phi}_O = \langle \boldsymbol{\phi}_i \rangle = \frac{1}{N} \sum_{i=1}^{N} \boldsymbol{\phi}_i, \tag{15}$$

for which $\boldsymbol{r}_O = (0,0)$. The Cartesian coordiantes of a point i is then determined based on its great-circle distance from the origin O. In particular, the x-coordinate of i is its (signed) great-circle distance from the point that has the same longitude φ_O as O and the same latitude θ_i as i itself. On the other hand, the y-coordinate of i is its (signed) great-circle distance from the point that has the same latitude θ_O as O and the same longitude φ_i as i itself. The great-circle distance is calculated using the "haversine" formula and, hence, the Cartesian coordinates of point i are given by

$$x_i = 2R \tan^{-1} \left(\frac{\cos \theta_i \sin \frac{\varphi_i - \varphi_O}{2}}{\sqrt{1 - \cos^2 \theta_i \sin^2 \frac{\varphi_i - \varphi_O}{2}}} \right), \tag{16}$$

$$y_i = R(\theta_i - \theta_O), \tag{17}$$

$$\tag{18}$$

with $R = 6,371,000$m being the Earth's radius.

References

1. Batty, M. *Cities and Complexity* (The MIT Press, Cambridge, 2005).

2. Bettencourt, L. M. A., Lobo, J., Helbing, D., Kühnert, C. & West, G. B. Growth, innovation, scaling, and the pace of life in cities. *P. Natl. Acad. Sci.* **104**, 7301–7306 (2007).

3. Bettencourt, L. M. A., Lobo, J., Strumsky, D. & West, G. B. Urban scaling and its deviations: Revealing the structure of wealth, innovation and crime across cities. *PLoS ONE* **5**, e13541 (2010).

4. Bettencourt, L. M. A. & West, G. B. A unified theory of urban living. *Nature* **467**, 912—-913 (2010).

5. Bettencourt, L. M. A. The origins of scaling in cities. *Science* **340**, 1438–1441 (2013).

6. Batty, M. A theory of city size. *Science* **340**, 1418–1419 (2013).

7. Batty, M. *The New Science of Cities* (The MIT Press, Cambridge, 2013).

8. Batty, M. & Longley, P. *Fractal Cities: A Geometry of Form and Function* (Academic Press, London, 1994).

9. Open Street Map project. URL https://www.openstreetmap.org/.

10. Jiang, B. A topological pattern of urban street networks: Universality and peculiarity. *Physica A* **384**, 647–655 (2007).

11. Barthélemy, M. & Flammini, A. Modeling urban street patterns. *Phys. Rev. Lett.* **100**, 138702 (2008).

12. Strano, E., Nicosia, V., Latora, V., Porta, S. & Barthélemy, M. Elementary processes governing the evolution of road networks. *Nat. Sci. Rep.* **2**, 296 (2012).

13. Barthélemy, M., Bordin, P., Berestycki, H. & Gribaudi, M. Self-organization versus top-down planning in the evolution of a city. *Nat. Sci. Rep.* **3**, 2153 (2013).

14. Gudmundsson, A. & Mohajeri, N. Entropy and order in urban street networks. *Nat. Sci. Rep.* **3** (2013).

15. Strano, E. *et al.* Urban street networks, a comparative analysis of ten European cities. *Environ. Plann. B* **40**, 1071–1086 (2013).

16. Louf, R. & Barthelemy, M. A typology of street patterns. *J. Roy. Soc. Interface* **11** (2014).

17. Porta, S., Crucitti, P. & Latora, V. The network analysis of urban streets: A dual approach. *Physica A* **369**, 853–866 (2006).

18. Stauffer, D. & Aharony, A. *Introduction to percolation theory* (Taylor & Francis, London, 1994).

19. Domb, C., Green, M. S. & Lebowitz, J. (eds.) *Phase transitions and critical phenomena*, vol. 1–20 (Academic Press, 1972–2001).

20. Stanley, H. E. Scaling, universality, and renormalization: Three pillars of modern critical phenomena. *Rev. Mod. Phys.* **71**, S358–S366 (1999).

21. Clark, C. Urban population densities. *J. Roy. Stat. Soc. A Gen.* **114**, 490–496 (1951).

22. Makse, H. A., Andrade, J. S., Batty, M., Havlin, S. & Stanley, H. E. Modeling urban growth patterns with correlated percolation. *Phys. Rev. E* **58**, 7054 (1998).

23. Crutchfield, J. P. & Young, K. Inferring statistical complexity. *Phys. Rev. Lett.* **63**, 105–108 (1989).

24. Crutchfield, J. P. Between order and chaos. *Nat. Phys.* **8**, 17–24 (2012).

25. Huynh, H. N., Pradana, A. & Chew, L. Y. The complexity of sequences generated by the arc-fractal system. *PLoS ONE* **10**, e0117365 (2015).

26. Ester, M., Kriegel, H.-P., Sander, J. & Xu, X. A density-based algorithm for discovering clusters in large spatial databases with noise. In *Proceedings of the Second International Conference on Knowledge Discovery and Data Mining*, KDD-96, 226—231 (1996).

27. URL https://www.transitlink.com.sg/.

28. URL https://mapzen.com/data/metro-extracts/.

29. URL http://www.movable-type.co.uk/scripts/latlo

Acknowledgements

Author contributions statement

HNH, CM and LYC conceived and designed the study. HNH devised the method of analysis and analysed the data. EM collected the bus stop data of all cities. HNH and EFL collected the remaining data. HNH wrote the manuscript. All authors reviewed the manuscript.

Additional information

Competing financial interests: The authors declare no competing financial interests.